Int J Thermophys (2009) 30:591–598
DOI 10.1007/s10765-008-0519-5

# Thermal Properties of GaN Films Grown on Si Substrates

**M. Cervantes-Contreras · C. A. Quezada-Maya · C. Mejía-García · M. López-López · G. González de la Cruz · M. Tamura**

Received: 13 October 2007 / Accepted: 21 September 2008 / Published online: 16 October 2008
© Springer Science+Business Media, LLC 2008

**Abstract** GaN films grown on Si substrates by molecular beam epitaxy with different nitridation times have been investigated. The GaN/Si structural and optical properties were evaluated by transmission electron microscopy, X-ray diffraction, atomic force microscopy, and photoluminescence. The effective thermal conductivity of the GaN/Si system was obtained using the photoacoustic technique, and from these results the nitridation time dependence of the interface thermal conductivity ($\eta$) can be evaluated using a two-layer model. An optimal nitridation time for which the GaN crystal quality can be improved was obtained. The variation of the parameter $\eta$ for different nitridation times can be related to the interface phonon scattering process by the presence of disorder at the GaN/Si interface.

**Keywords** GaN/Si heterostructures · Molecular beam epitaxy · Nitridation time · Photoacoustic technique · Thermal conductivity

M. Cervantes-Contreras (✉)
Departamento de Matemáticas, Unidad Profesional Interdisciplinaria de Biotecnología-Intituto Politécnico Nacional, Ticoman, México, D.F. 07340, México
e-mail: cecontreras@ipn.mx

C. A. Quezada-Maya · C. Mejía-García
Escuela Superior de Física y Matemáticas, Instituto Politécnico Nacional, Edif. 9 UPALM, Av. IPN sn, México, D.F. 07738, México

M. López-López · G. González de la Cruz · M. Tamura
Physics Department, Centro de Investigación y de Estudios Avanzados del IPN, Apartado Postal 14-740, México, D.F. 07000, México

## 1 Introduction

Large efforts have been exercised in order to obtain high-quality GaN films. The first stage of growth conditions determines the characteristics of the subsequent GaN epitaxial layers. In particular, the nitridation of the substrate surface notably affects the properties of the GaN overlayers, such as surface morphology, and structural and optical properties [1–3]. Thus, the study of the initial substrate nitridation can have significant impact.

The heteroepitaxy of GaN on Si substrates has attracted attention due to important technological application [4]. The increase in the GaN crystal quality has made possible the fabrication of microelectronic devices with improved performance [5]. Efficient heat removal is particularly relevant in the performance of these devices. Therefore, a good knowledge of the thermal properties of GaN/Si is needed. For example, the study of the thermal conductivity of different systems [6] has been a subject of significant interest. This parameter plays an important role for the understanding of heat transport phenomena in various devices. To address the problem of heat flow in a heterostructure, one has to take into account the influence of structural defects, since these may contribute sensitively to the effective thermal conductivity of the system [7].

However, little has been reported on the effects of nitridation of the substrate surface and the thermal properties of the GaN/Si heterostructure. In this study we have studied the influence of structural defects on the GaNSi thermal conductivity. Changes in the GaN/Si structural and optical characteristics were induced by varying the Si substrate nitridation time.

## 2 Experimental Procedure

GaN films were grown in a conventional molecular beam epitaxy (MBE) system equipped with a plasma source for the production of active nitrogen species. We employed Si substrates with (111) orientation. The native oxide on the substrate surface was etched in a buffered HF solution, then it was loaded into the MBE system and was thermally cleaned at 1250 °C for 5 min. Then, the substrate temperature was lowered to 800 °C, and the N source was opened for a time $t_N$ with a nitrogen gas flow rate of 2 sccm and a plasma power of 350 W. Immediately after the nitridation process, GaN growth was carried out at the same substrate temperature employing a Ga-cell temperature of 1040 °C. The GaN growth time was fixed at 2 h resulting in films of around 200 nm. We prepared different samples varying the nitridation time $t_N$ from 0 min to 60 min.

The structural characteristics of the samples were evaluated by transmission electron microscopy (TEM) at 200 keV, X-ray diffraction (XRD), and atomic force microscopy (AFM). The optical properties of the samples were investigated by photoluminescence (PL) at 14 K, and the 325 nm line of a He–Cd laser was used as an excitation source. For the thermal characterization we employed the open photoacoustic technique, which has been described in detail elsewhere [8]. Briefly, this technique consists of mounting the sample directly on a cylindrical electrect microphone and exposing it to a modulated light beam. We used a 40 mW argon laser mechanically

modulated with a chopper and uniformly focused onto the sample. As a result of the periodic heating of the sample by the absorption of the modulated light, the pressure in the microphone chamber oscillates at the chopping frequency. A lock-in amplifier is then used to record the acoustic signal detected in the microphone. Since the magnitude of the periodic pressure fluctuations in the cell is proportional to the temperature fluctuations in the sample (thermal waves), there is a close relation between the strength and the phase of the acoustical signal and the thermal parameters of the material. Therefore, from the photoacoustic signal, it is possible to obtain the effective thermal diffusivity of the heterostructure at room temperature, and as will be explained below, the interface thermal conductivity between the two layers of GaN and Si.

## 3 Results and Discussion

First we will discuss the effect of the different nitridation times on the structural properties of the samples. We observed that even in the samples with no intentional nitridation ($t_N = 0$) a SiN amorphous layer was formed at the interface independent of the Si substrate orientation. We show in Fig. 1a a high-resolution cross-sectional TEM (HRXTEM) image of the interface region corresponding to GaN grown on Si(111) for $t_N = 0$. In this case, $t_N = 0$ means that GaN growth was started by the simultaneous supply of Ga and N just after substrate thermal cleaning in the MBE chamber. We clearly note from Fig. 1a that a non-uniform ∼2 nm thick amorphous SiN layer is formed at the interface. This result suggests that the Si surface easily reacts with nitrogen at the initial stage of GaN growth, resulting in the SiN layer formation. In fact, some authors have previously shown the formation of amorphous SiN on Si substrates with no special nitridation procedures [9,10]. The residual nitrogen gas in the

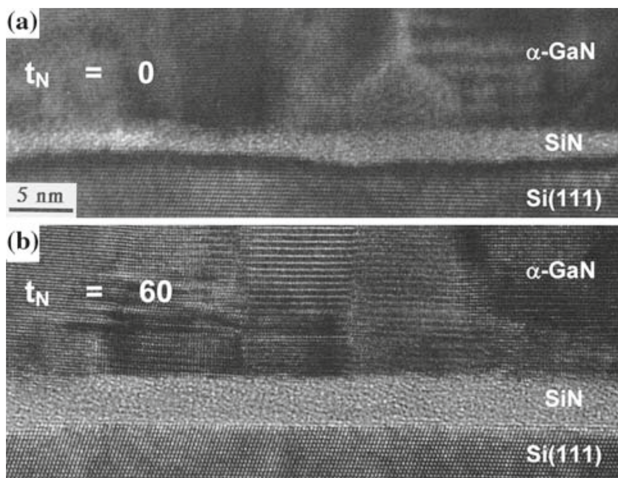


**Fig. 1** HRXTEM micrographs of the interface region of GaN films grown on Si(111) substrates treated with nitridation times of (a) 0 min and (b) 60 min, observed from the $[1\bar{1}0]$ direction of Si

growth chamber during the thermal cleaning procedure could also contribute to the SiN formation on Si substrates with $t_N = 0$.

When we employed an intentional nitridation process, we observed a small increase in the SiN thickness. However, the most relevant change for times $t_N$ longer than a few minutes is the formation of a flatter and uniform amorphous SiN layer at the Si surface. In Fig. 1b is shown an HRXTEM image of the interface region corresponding to GaN/Si(111) with $t_N = 60$ min. The micrograph reveals the formation of an ∼3.5 nm thick amorphous SiN layer having a very sharp interface with the Si substrate, and with the GaN film.

For all $t_N$ employed in this study, we found from transmission electron diffraction patterns that hexagonal GaN films were obtained with the following epitaxial relationships: [0001]GaN//[111]Si and $[11\bar{2}0]$GaN//$[1\bar{1}0]$Si.

Figure 2 shows on the right-hand vertical axis the root-mean-square (RMS) surface roughness value as a function of the nitridation time. This figure confirms the smoother GaN surface obtained for $t_N = 2$ min with an RMS of 7 nm. The insets in Fig. 2 show AFM images for samples with nitridation times of (a) 0 min, (b) 2 min, and (c) 60 min. From Fig. 2a, we note that the high RMS value of 146 nm for 0 min nitridation time is caused by large grains formed in the film. To obtain additional information on the

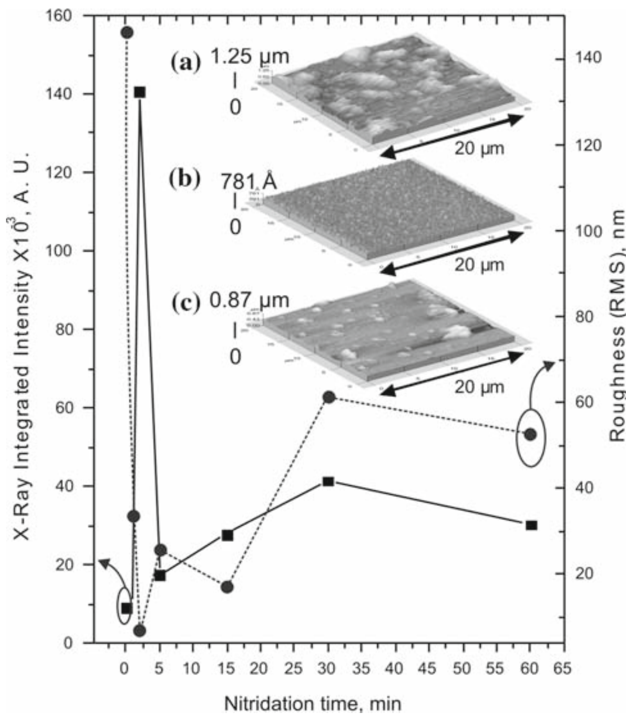


**Fig. 2** Plot of RMS roughness (right-hand vertical axis) as obtained by AFM measurements, and X-ray integrated intensity (left-hand vertical axis) from the GaN(0002) reflection peak as a function of the Si(111) substrate nitridation time. Insets show AFM images of samples with nitridation times of (a) 0 min, (b) 2 min, and (c) 60 min

structural properties of the samples, XRD measurements were performed. Figure 2 shows the integrated XRD intensity (left-hand vertical axis) of the (0002) GaN reflection peak normalized to that of the (004) Si peak from the substrate, as a function of the nitridation time. We note that a very low XRD intensity is obtained for the film grown with no targeted nitridation time. As $t_N$ is increased, the XRD intensity also increases showing a maximum at $t_N = 2\,\text{min}$. For longer nitridation times, the XRD intensity decreases indicating degradation in the structural properties.

It is surprising that epitaxial growth can be obtained despite the relatively thick amorphous layer (∼3 nm) at the interface between GaN and Si. A possible explanation might be the presence of nucleation sites like small crystalline regions [11] or holes in the SiN via which the crystalline information is provided. The behavior of the structural properties of the GaN films as a function of $t_N$ suggests that the density of these nucleation sites is strongly dependent on the nitridation time. Moreover, we have found that there is an optimal nitridation time (2 min) for which the nucleation sites density yields a lower amount of defects.

Next we present the optical characteristics of the films as studied by PL at 14 K. In the PL spectra for nitridation times from 0 min to 60 min, outstanding tree peaks can be seen centered at 2.2 eV, 3.1 eV, and 3.5 eV. The very broad band at 2.2 eV is known as yellow luminescence, and is related to deep levels in the band gap. The one at ∼3.1 eV could be due to donor–acceptor pair transitions, and the one at 3.5 eV is related to excitonic emission [12].

Figure 3 shows on the right-hand vertical axis the integrated intensity of the excitonic emission normalized to that of the yellow luminescence, as a function of the nitridation time. We note that the highest value of the normalized integrated PL intensity is obtained for the film grown with $t_N = 2\,\text{min}$. The yellow luminescence will decrease the efficiency of the devices, especially for devices operating at room temperature. Therefore, this result shows additional evidence of an improvement in material quality for GaN at $t_N = 2\,\text{min}$. The presence of the SiN layer and crystal defects in the GaN/Si heterostructure is expected to have a large effect on the heat transport. Here the photoacoustic technique [7] is a powerful tool to determine the effective thermal conductivity of the GaN/Si system.

Assuming an optically opaque sample (i.e., all the incident light is absorbed at the surface and converted into heat), and solving the thermal diffusion equation for the effective semiconductor material, which in this study represents the GaN/Si heterostructure, the microphone output phase can be written as [8]

$$\Delta\varphi = -\arctan\left[\frac{\tan\sqrt{f/f_c}}{\tanh\sqrt{f/f_c}}\right] - \frac{\pi}{2}, \tag{1}$$

where $f_c = \alpha/\pi d^2$ is the characteristic thermal frequency at which the sample responds to an external perturbation, $\alpha$ the effective thermal diffusivity, $d$ the total thickness of the sample, and $f$ is the chopper frequency.

Considering that the GaN thickness ($d_{GaN} \sim 200\,\text{nm}$) is much smaller than the Si substrate thickness ($d_{Si} \sim 400\,\mu\text{m}$), the effective thermal diffusivity is given by the following relationship [7]:

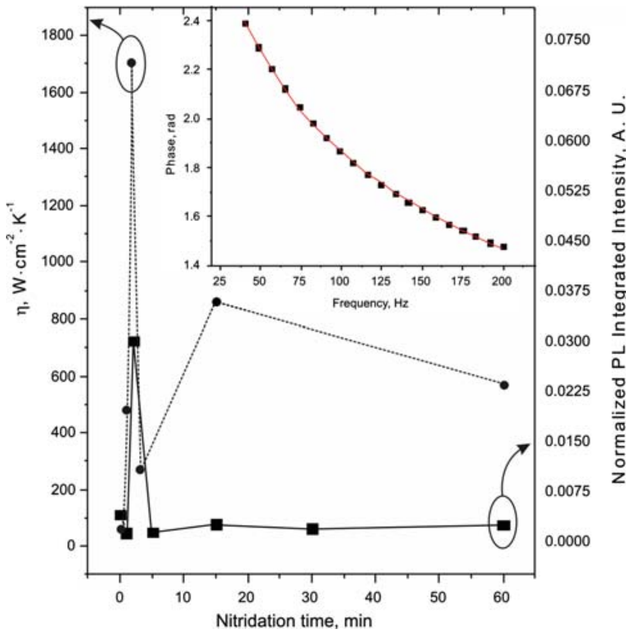


**Fig. 3** Plot of the integrated 14K-PL intensity of the excitonic emission normalized to that of the yellow luminescence (right-hand vertical axis) and GaN/Si(111) interfacial thermal conductivity ($\eta$) (left-hand vertical axis) as a function of the substrate nitridation time. Inset shows the photoacustic signal phase as a function of the modulation frequency for the sample with 60 min nitridation time

$$\frac{1}{\alpha} = \frac{1}{\alpha_{\text{Si}}}\left(\frac{2\kappa_{\text{Si}}}{\eta d_{\text{Si}}} + 1\right), \tag{2}$$

where $\alpha_{\text{Si}}$ and $\kappa_{\text{Si}}$ are the Si thermal diffusivity and thermal conductivity, respectively. The interfacial thermal conductivity $\eta$ is given as the ratio of the heat flowing across the interface and the difference of temperature between the two materials, i.e.,

$$-\kappa_1 \frac{\mathrm{d}T_1(x,t)}{\mathrm{d}x} = \eta\,[T_1(x,t) - T_2(x,t)] \quad \eta > 0. \tag{3}$$

The temperatures $T_i(x,t)$, $i = 1, 2$ represent the solution of the heat diffusion equation in Si and GaN, respectively. Physically, the parameter $\eta \to \infty$, represents perfect thermal contact, and because the heat flux is continuous at the interface, the temperature distribution must be continuous at the interface. On the contrary, for finite $\eta$, the temperature fluctuation is discontinuous across the boundary. A finite interfacial thermal conductivity between different constituent materials in a composite may originate from disorder caused by a combination of poor mechanical or chemical adherence at the interface, and a thermal expansion mismatch. Therefore, dispersive effects such as scattering of phonons can strongly influence the heat flow in a system. Direct evidence of the interfacial thermal conductivity effects for helium-solid systems over a wide

range of temperatures was provided by Swartz and Pohl [13], and more recently for AlN/diamond systems [6].

It is worth noting that, in Eq. 2, defects at the interface region and the thin SiN layer contribute to the effective thermal diffusivity of the GaN/Si heterostructure through the parameter $\eta$. Therefore, by fitting the experimental data for the photoacoustic cell signal phase as a function of the modulation frequency with Eq. 1, we can obtain the effective thermal diffusivity $\alpha$, and the interface thermal conductivity $\eta$ between Si and GaN by means of Eq. 2.

In the inset of Fig. 3, the photoacoustic signal phase measured in the above-stated configuration is shown as a function of the modulation frequency for a GaN/Si(111) sample with $t_N = 60\,\text{min}$. The solid line represents the fit of the experimental data to Eq. 1. As a result of this fit, an effective thermal diffusivity $\alpha = 0.77\,\text{cm}^2 \cdot \text{s}^{-1}$ was extracted, and an interfacial thermal conductivity of $\eta$=571.17 $\text{W} \cdot \text{cm}^{-2} \cdot \text{K}^{-1}$ was obtained, with the Si thermal parameters $\alpha_{\text{Si}}$ and $\kappa_{\text{Si}}$ taken from Ref. [14]. This procedure was carried out for the samples with different nitridation times. The obtained interfacial thermal conductivity as a function of the nitridation time is shown in Fig. 3. As can be observed, small values of $\eta$ were obtained at short nitridation times, but $\eta$ shows a maximum for the sample with $t_N = 2\,\text{min}$. For this sample $\eta = 1710.96\,\text{W} \cdot \text{cm}^{-2} \cdot \text{K}^{-1}$. Above $t_N = 2\,\text{min}$, the interfacial thermal conductivity decreases, reaching similar values as the initial ones. The variation of the parameter $\eta$ for different nitridation times can be associated with phonon scattering caused by the presence of disorder in the heterostructure [13]. Thus, according to Fig. 3, a significant suppression of phonon scattering occurs in the sample prepared with $t_N = 2\,\text{min}$. This fact suggests that this sample contains considerable less microscopic disorder, in agreement with the TEM, XRD, AFM, and PL results of Figs. 1–3.

## 4 Conclusions

In summary, we carried out a study of structural, optical, and thermal properties of GaN/Si heterostructures as a function of the substrate nitridation time. By varying the nitridation time, changes in the structural and optical properties of GaN/Si heterostructures were obtained. We observed a reduction of the amount of structural defects in the GaN films for a nitridation time of $t_N = 2\,\text{min}$. At this nitridation time, weaker yellow luminescence is the result. The thermal resistance of the interfacial region strongly depends on the nitridation conditions. The thermal conductivity at the GaN/Si interface presented a maximum value for the optimal nitridation time.

**Acknowledgments** This work has been partially supported by Consejo Nacional de Ciencia y Tecnologia (Conacyt), Mexico. The authors would like to thank Rogelio Fragoso, Erasmo Gómez, and Marcela Guerrero for technical assistance.

## References

1. A. Kikuchi, H. Hoshi, K. Kishino, Jpn. J. Appl. Phys. **33**, 688 (1994)
2. K. Uchida, A. Watanabe, F. Yano, M. Kouguchi, T. Tanaka, S. Minagawa, J. Appl. Phys. **79**, 3487 (1996)

3. K.S. Kim, K.Y. Lim, H.J. Lee, Semicond. Sci. Technol. **14**, 557 (1999)
4. S. Pal, C. Jacob, Bull. Mater. Sci. **27**, 501 (2004)
5. R. Behtash, H. Tobler, P. Marschall. A. Schurr, H. Leier, Y. Cordier, F. Semond, F. Natali, J. Messies, IEE Electron. Lett. **39**, 626K (2003)
6. K. Jagannadham, H. Wang, J. Appl. Phys. **91**, 1224 (2001)
7. N. Muñoz, G. Gonzalez de la Cruz, Y. Gurevich, G.N. Logvinov, M.N. Kasyanchuck, Phys. Stat. Sol. B **220**, 781 (2000)
8. M. Marquezini, N. Cella, A. Manzanares, H. Vargas, L.C.M. Miranda, Meas. Sci. Technol. **2**, 396 (1991)
9. Y. Hiroyama, M. Tamura, Jpn. J. Appl. Phys. **37**, L630 (1998)
10. H. Lahreche, P. Vennegues, O. Tottenreau, M. Laugt, P. Lorenzini, M. Leroux, B. Beaumont, P. Gibart, J. Cryst. Growth **217**, L630 (2000)
11. Y. Nakada, I. Aksenov, H. Okumura, Appl. Phys. Lett. **73**, 827 (1998)
12. J. Menniger, U. Jahn, O. Brandt, H. Yang, K. Ploog, Phys. Rev. B **53**, 1881 (1996)
13. E.T. Swartz, R.O. Pohl, Rev. Mod. Phys. **61**, 605 (1989)
14. Y.S. Touloukian, E.H. Buyco, eds., In *Thermal Conductivity of Nonmetallic Solids, Thermophysical Properties of Matter*, (IFI/Plenum, New York, 1970)